

Electronic Supplementary Information

Effects of strongly aggregated silica nanoparticles on interfacial behaviour of water bound to lactic acid bacteria

Vladimir M. Gun'ko,^{*,a} Vladimir V. Turov,^a Tetyana V. Krupskaya,^a Magdalina D. Tsapko,^b Jadwiga Skubiszewska-Zięba,^c Barbara Charmas,^c and Roman Leboda^c

Hydrophobization of silica gel

To modify silica gel Sipernat 50 (Si50) (Evonik), surface functionalities were attached by silylation with octadecyldimethylchlorosilane (ODDMCS). The silylation reaction was carried out in dry toluene (60 ml) using 9 g of Si50 and 7.237 g of silane. Before the reaction, Si50 was heated at 150 °C in vacuum (10^{-3} atm) for 4 h. After cooling to 100 °C, the toluene solution of ODDMCS was added, and the reaction mixture was maintained at 105 °C for 14 h. Silylated Si50 (Si50s) was filtered and washed with toluene and methanol.

Textural and structural characteristics

To analyze the textural characteristics of initial and silylated silica gels degassed for several hours, low-temperature (77.4 K) nitrogen adsorption–desorption isotherms were recorded using a Micromeritics ASAP 2405N adsorption analyzer. The specific surface area (S_{BET}) was calculated according to the standard BET method.¹ The total pore volume V_p was evaluated from the nitrogen adsorption at $p/p_0 \approx 0.99$, where p and p_0 denote the equilibrium and saturation pressure of nitrogen at 77.4 K, respectively.² The nitrogen desorption data were used to compute the pore size distributions (PSD, differential $f_V(R) \sim dV_p/dR$ and $f_S(R) \sim dS/dR$) using a self-consistent regularization (SCR) procedure under non-negativity condition ($f_V(R) \geq 0$ at any pore radius R) at a fixed regularization parameter $\alpha = 0.01$ with a complex pore model using cylindrical (C) pores and voids (V) between spherical nonporous nanoparticles packed in random aggregates for initial and silylated silica gels.^{3,4} The differential PSD with respect to pore volume $f_V(R) \sim dV/dR$, $\int f_V(R)dR \sim V_p$ were re-calculated to incremental PSD (IPSD) at $\Phi_V(R_i) = (f_V(R_{i+1}) + f_V(R_i))(R_{i+1} - R_i)/2$ at $\sum \Phi_V(R_i) = V_p$. The differential $f_S(R)$ functions were used to estimate the deviation of the pore shape from the model as follows

$$\Delta w = \left(S_{\text{BET}} / \int_{R_{\text{min}}}^{R_{\text{max}}} f_S(R) dR \right) - 1, \quad (\text{S1})$$

where R_{\max} and R_{\min} are the maximal and minimal pore radii, respectively.⁴ The $f_V(R)$ and $f_S(R)$ functions were also used to calculate contributions of nanopores (V_{nano} and S_{nano} at $0.35 \text{ nm} < R < 1 \text{ nm}$), mesopores (V_{meso} and S_{meso} at $1 \text{ nm} < R < 25 \text{ nm}$), and macropores (V_{macro} and S_{macro} at $25 \text{ nm} < R < 100 \text{ nm}$). The average values of the pore radii were determined with respect to the pore volume and specific surface area as the ratio of the first and zero moments of the corresponding distribution functions

$$\langle R_V \rangle = \frac{\int_{R_{\min}}^{R_{\max}} R f_V(R) dR}{\int_{R_{\min}}^{R_{\max}} f_V(R) dR}, \quad (\text{S2})$$

$$\langle R_S \rangle = \frac{\int_{R_{\min}}^{R_{\max}} R f_S(R) dR}{\int_{R_{\min}}^{R_{\max}} f_S(R) dR}. \quad (\text{S3})$$

Additionally, the PSD functions were calculated using nonlocal density functional theory (NLDFT) method⁵ using equilibrium models of cylindrical pores in silica (for silica gel).

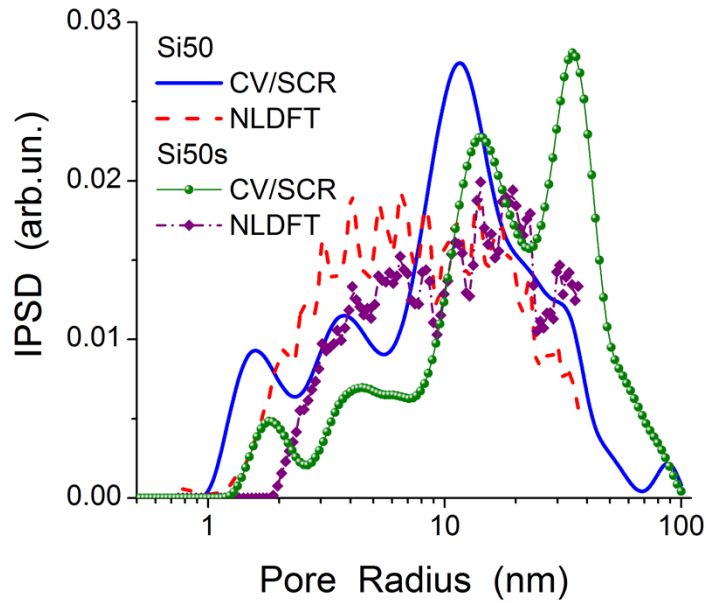


Fig. S1 Incremental pore size distributions for initial (Si50) and silylated (Si50s) silica gels calculated using the NLDFT and CV/SCR methods.

Silica gel Si50 studied is characterized by a wide pore size distribution (Fig. S1) with main contributions of mesopores (Table S1, S_{meso} and V_{meso}) and macropores (S_{macro} and V_{macro}). Therefore, the average radii of pores with respect to the pore volume $\langle R_V \rangle$ and specific surface area $\langle R_S \rangle$ are relatively large for initial and modified silica gels. The surface of initial and silylated silica gels is not smooth. This leads to relatively great errors of the CV/SCR model of pores (Table S1, Δw). Note that observed increase in the macroporosity of Si50s (S_{macro} and V_{macro}) can be caused by certain changes in

the structure of silica gel microparticles (resulting in broadening of macropores, Fig. S1) during the modification treatment processes and enhanced aggregation of the particles.

Table S1 Textural characteristics of initial and silylated Sipernat 50.

Sample	S_{BET} (m^2/g)	S_{nano} (m^2/g)	S_{meso} (m^2/g)	S_{macro} (m^2/g)	V_{p} (cm^3/g)	V_{nano} (cm^3/g)	V_{meso} (cm^3/g)	V_{macro} (cm^3/g)	$\langle R_{\text{V}} \rangle$ (nm)	$\langle R_{\text{S}} \rangle$ (nm)	Δw
Si50	503	2	488	13	1.292	0.001	1.114	0.177	13.7	5.7	0.210
Si50s	261	0	234	27	1.217	0.0	0.756	0.461	22.9	10.2	0.099

Note. Si50 and Si50s are the initial and silylated silica gels, respectively.

Thermogravimetry data (Fig. S2) and FTIR spectrum (Fig. S3) show that the degree of silylation of Si50 is high, since the weight loss related to elimination of organic groups of silane functionalities attached to Si50s is about 15 wt.% (Fig. S2). The adsorption of water onto Si50s is lower than that onto Si50 (see weight loss at $T < 200$ °C).

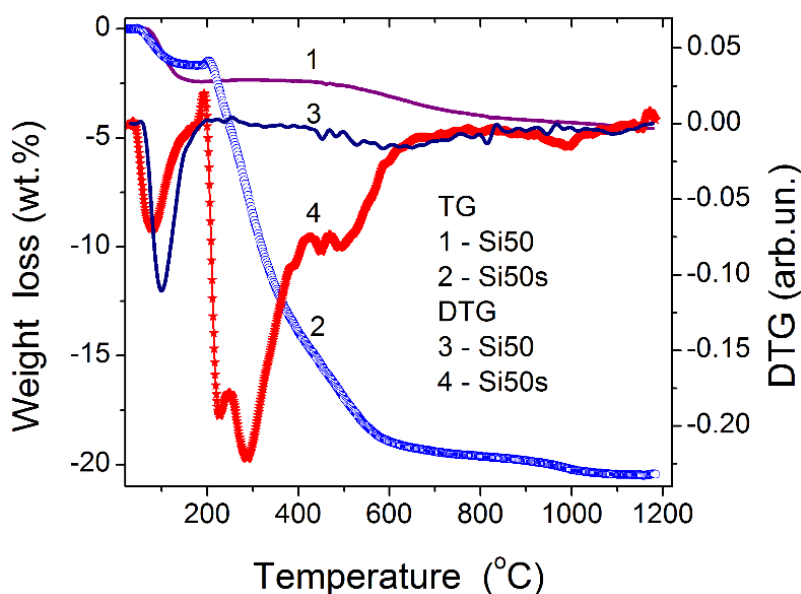


Fig. S2 Thermogravimetry (TG) measurements (Derivatograph C, Paulik, Paulik and Erdey, MOM, Budapest) of weight loss (TG) and differential TG (DTG) vs. temperature for initial (Si50) and silylated (Si50s) Sipernat 50.

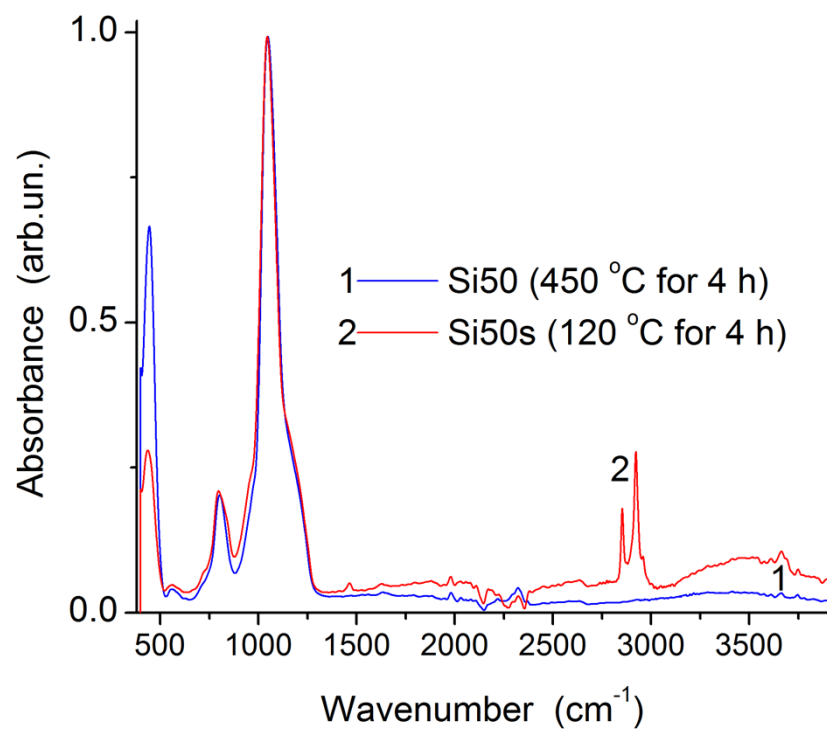


Fig. S3 Fourier transform infrared spectroscopy (FTIR) with attenuated total reflection (ATR) applied to initial (curve 1, preheated at 450 °C for 4 h) and silylated (curve 2, preheated at 120 °C for 4 h) Sipernat 50 (FTIR Nicolet 8700, Thermo Scientific, used diamond crystal).

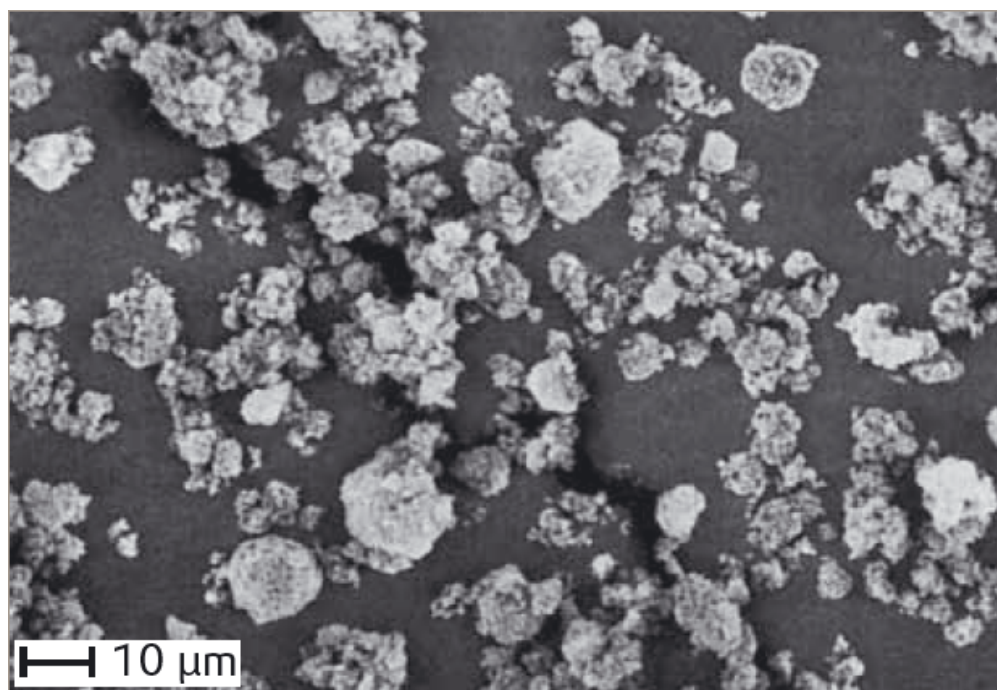
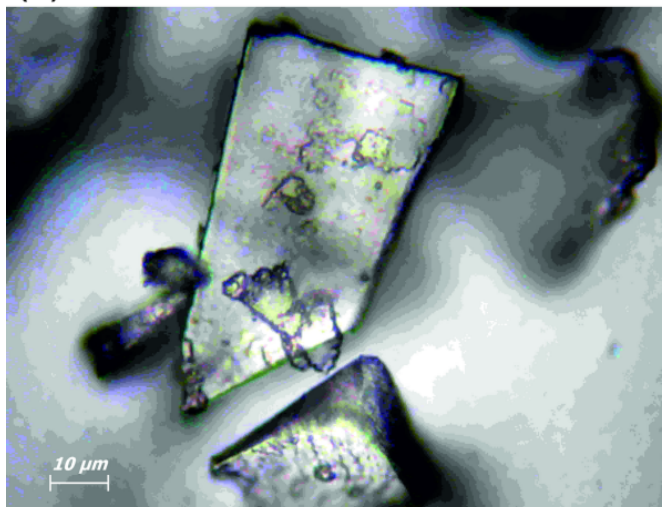
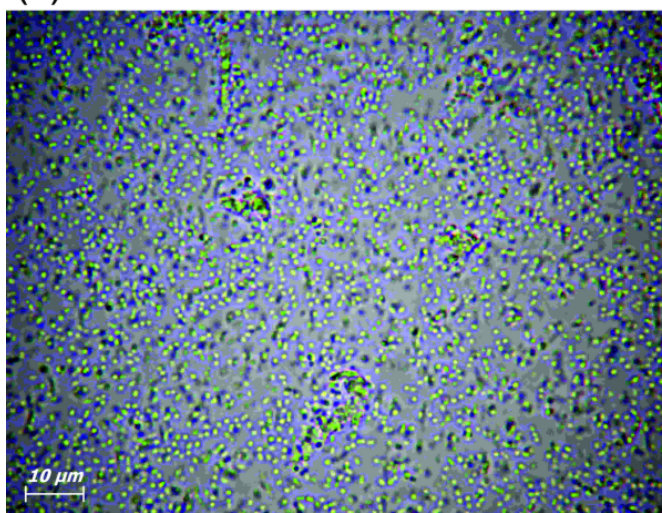


Fig. S4 Microphoto of silica TS 100.⁶

(a)



(b)



(c)

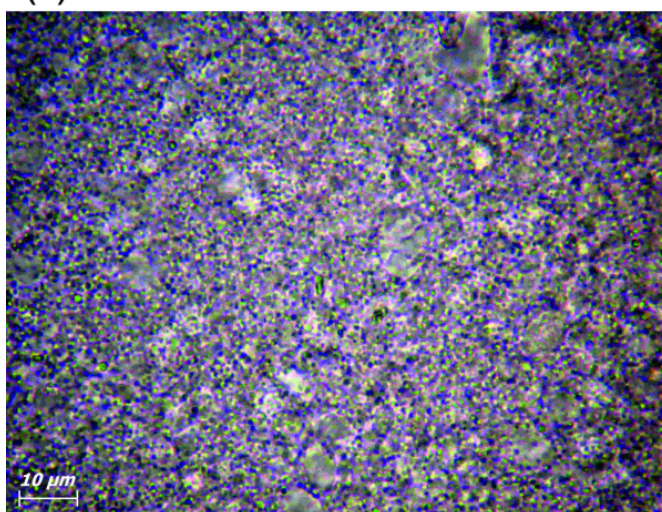


Fig. S5 Microphotos of (a) freeze-dry LAB, (b) aqueous suspension of LAB, and (c) a mixture of hydrated LAB with TS 100 (scale bar 10 μm).

The chemical shift of proton resonance *vs.* temperature, $\delta_H(T)$, depends on the number of possible configurations of water molecules in the hydrogen bonds network. This number depends on the average number of the hydrogen bonds $\langle n_{HB} \rangle$, according to the entropy definition $S \approx -k_B \ln n_{HB}$. Therefore, the temperature derivative of the measured fractional chemical shift⁷

$$-\left(\frac{\partial \ln \delta(T)}{\partial T}\right)_p = -\left(\frac{\partial \ln \langle n_{HB} \rangle}{\partial T}\right)_p \approx \left(\frac{\partial S}{\partial T}\right)_p \quad (\text{S4})$$

should be proportional to the constant pressure specific heat $C_p(T)$ ($C_p = T(\partial S/\partial T)_p$). Here the $T(\partial \ln \delta(T)/\partial T)_p$ functions are compared for water bound to LAB differently hydrated in various dispersion media (Fig. S6).

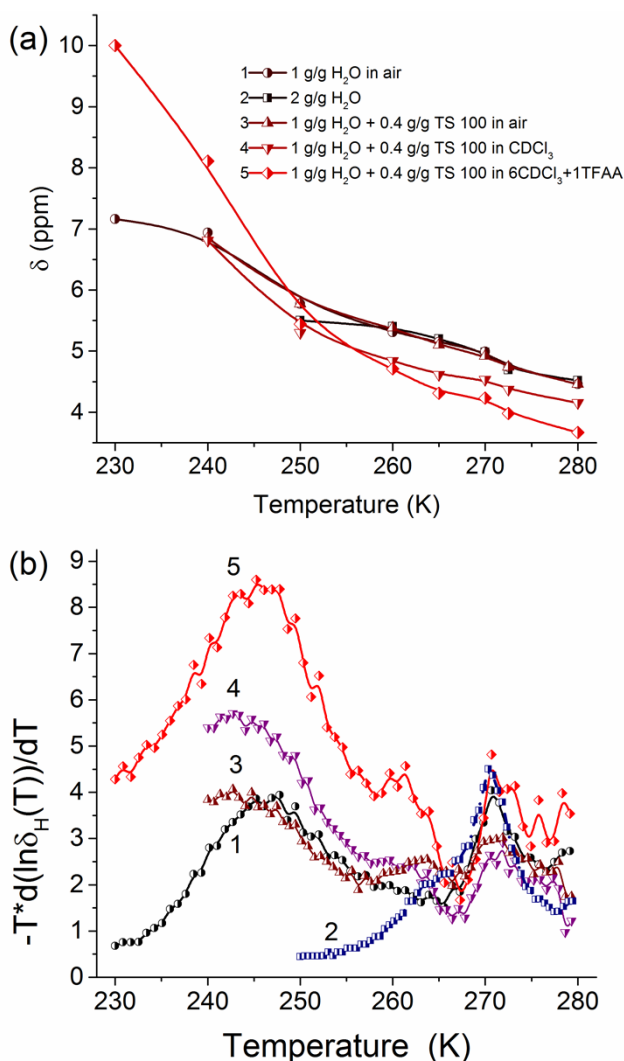


Fig. S6 (a) Chemical shift for main ¹H NMR signal of water bound to LAB and (b) corresponding functions $-T(\partial \ln \delta(T)/\partial T)_p$ *vs.* temperature.

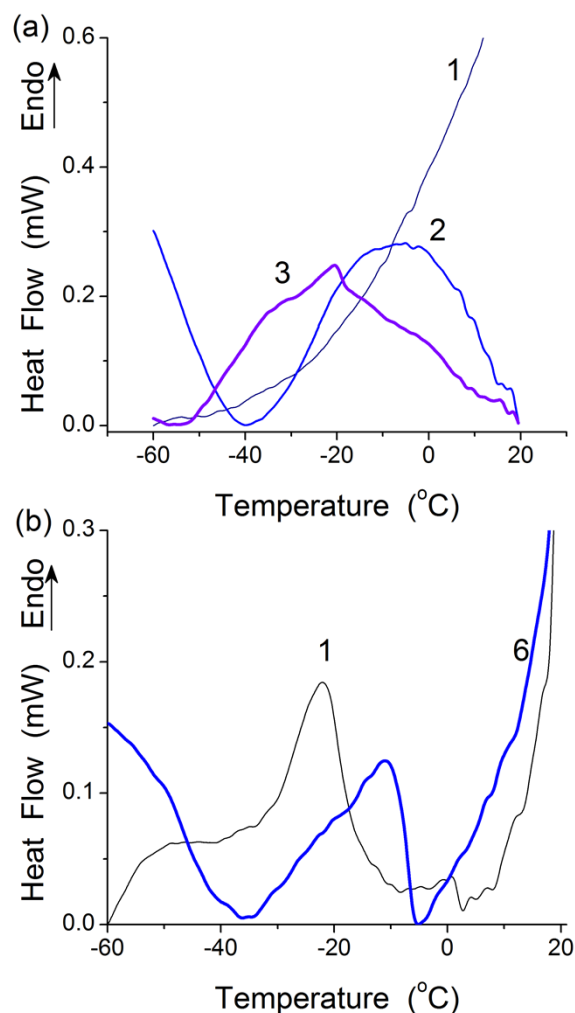


Fig. S7 DSC thermograms for heating of LAB at various amounts of added water: (a) 0 (curves 1), 0.1 (2), and 0.2 (3) g/g (details in Table 2, Fig. 3b), and (b) LAB interacting with Si50s at $C_{Si50s} = 0.3$ (curve 1) and 0.5 (curve 6) g/g (see Fig. 3c) in various surroundings shown in Table 3.

Notes and references

^a *Chuiiko Institute of Surface Chemistry, General Naumov Street 17, 03164 Kiev, Ukraine. Fax: 38044 4243567; Tel: 38044 4229627; e-mail: vlad_gunko@ukr.net;*

^b *Faculty of Chemistry, Taras Shevchenko University, 01030 Kiev, Ukraine. e-mail: nmrlab2007@ukr.net;*

^c *Faculty of Chemistry, Maria Curie-Skłodowska University, 20-031 Lublin, Poland. e-mail: jskubisz@o2.pl.*

- 1 A.W. Adamson and A.P. Gast, *Physical Chemistry of Surfaces*. 6th ed. Wiley, New York, 1997.
- 2 S.J. Gregg and K.S.W. Sing, *Adsorption, Surface Area and Porosity*. Second ed. Academic Press, London, 1982.
- 3 V.M. Gun'ko, *Applied Surface Science*, 2014, **307**, 444.
- 4 V.M. Gun'ko and V.V. Turov, *Nuclear Magnetic Resonance Studies of Interfacial Phenomena*, CRC Press, Boca Raton, 2013.
- 5 A.V. Neimark and P.I. Ravikovitch, *Microporous and Mesoporous Materials*, 2001, **44/45**, 697.
- 6 Evonik Ind., ACEMATTR – Matting agents for the coatings industry, *Technical Bulletin Fine Particles*, 2014, No 21.
- 7 (a) F. Mallamace, C. Corsaro, M. Broccio, C. Branca, N. González-Segredo, J. Spooren, S.-H. Chen and H.E. Stanley, *Proc. Natl. Acad. Sci. USA*, 2008, **105**, 12725; (b) V.V. Turov, V.M. Gun'ko, V.I. Zarko, O.V. Goncharuk, T.V. Krupska, A.V. Turov, R. Lebeda and J. Skubiszewska-Zięba, *Langmuir*, 2013, **29**, 4303.